Hindawi
Wireless Communications and Mobile Computing
Volume 2022, Article ID 3221210, 11 pages
https://doi.org/10.1155/2022/3221210

Research Article

Cloud Computing Based on Big Data-Driven Robot Walking Route and Real-Time Positioning Intelligent Determination

Yunlong Yi,[1] **Ying Guan**,[1] **and Xiangbin Meng**[2]

[1]*School of Information, Shenyang Institute of Engineering, Shenyang, 110136 Liaoning, China*
[2]*School of Automation, Shenyang Institute of Engineering, Shenyang, 110136 Liaoning, China*

Correspondence should be addressed to Yunlong Yi; yiyl@sie.edu.cn

Received 24 June 2022; Revised 23 August 2022; Accepted 5 September 2022; Published 23 September 2022

Academic Editor: Kapil Sharma

With the continuous development of technologies such as sensors, computers, and artificial intelligence, intelligent mobile robots with thinking, perception, and dynamics functions are widely used in military, political, and scientific research. Its development has had a significant impact on national defense, society, economy, science, and technology and has become a strategic research goal in the high-tech field of various countries. Robot positioning technology is one of the key research technologies for portable robots, and reliable posture is the key prerequisite for completing various tasks. This article aims to study the robot walking route driven by big data and the intelligent determination of real-time positioning based on cloud computing. This paper proposes an active general positioning algorithm based on real-time positioning function, which can improve the convergence speed and robustness of general positioning when different map scenes do not have clear geometric features and contain map noise. The most basic requirement for robots to perform autonomous operations is to have reliable positioning performance. The experimental results in this paper show that dynamic global positioning and adaptive behavior tracking are effective. Compared with the traditional algorithm, the improved algorithm increases the convergence speed of the global layout by 41.59%.

1. Introduction

An intelligent mobile robot is a comprehensive system that integrates environmental perception, dynamic decision-making and planning, behavior control, and execution. Over the years, with the development of science and technology, the improvement of computer performance, and the fusion of artificial intelligence and control theory, mobile robotics, as an interdisciplinary subject, has involved multiple research fields, which has attracted more and more public attention. In this field, we mainly focus on the "motion" characteristics of mobile robots and combine many functions, such as perception of environmental and self-state, execution and control of actions, dynamic planning, and decision-making. The research on mobile robots began in the late 1960s. From 1966 to mid-1972, researchers at the Stanford Research Institute developed a mobile robot called "Shakey" whose basic functions include perception, environment modeling, and motion design. At the same time, the Soviet Union and the United States also developed the first unmanned lunar rover. In 1997, the American rover Soiner who successfully landed on Mars took as many as 500 photos related to the Martian landscape and sent them back to Earth. This should be a major success in the actual application of wheeled robots. Since its establishment, mobile robots have made considerable progress in engines and architectures, integrating multi-sensor information, positioning, route planning, and navigation monitoring and control. These technologies can be applied not only in the military field but also in private and scientific research fields. Especially in the private sector, portable robot technology can be used to control the automatic and semi-autonomous driving of vehicles to improve safety, and it can be applied to smart wheelchairs to improve the elderly and the disabled quality of life. In the long run, these technologies can also benefit from disaster search and rescue, emergency rescue, and other dangers and difficult opportunities faced by humans. This paper aims to study the robot walking route driven by big data and the intelligent determination of real-time positioning based on cloud computing,

in order to make a certain contribution to the real-time positioning of robots.

For a series of related research on artificial intelligence robot technology, my country has also successively carried out major special projects of the "15th Five-Year Plan." For example, many studies, such as robots based on bionics, service-oriented application robots, and robots that can operate in hazardous environments, have produced many effective results. During the 863 Program, Tsinghua University developed an intelligent robot platform that has multifunctional functions that can be used for outdoor experiments. As the first Frontier-ITM mobile autonomous robot to represent a Chinese university in the RoboCup medium-sized football match, it was independently developed by Shanghai Jiao-tong University. Shanghai Jiao-tong University and Harbin Institute of Technology have also jointly developed a hotel service robot, which has been exhibited at industrial fairs in recent years. At the same time, in the RoboCup China Open Home Service Robot Competition in recent years, home service robots such as "Jiao-long" from Shanghai Jiao-tong University, "Ke-jia" from University of Science and Technology of China, and "Amanda" from Shanghai University have all achieved success and great improvement. They have some basic functions, such as environment modeling, independent installation, automatic navigation, face recognition, voice interaction, and object capture. Among related mobile robot technologies, positioning technology has always been one of the most basic technologies in the research field. For autonomous robot mobile devices, reliable positioning results are the most basic condition for accomplishing various tasks.

Rezaee A uses an algorithm that continuously assigns PID coefficients based on an online algorithm, depending on the system characteristics based on fuzzy logic. The welding robot used in this system is used to weld oil and gas pipelines. Place the robot on the pipe and move it to weld. The motor is used to move the robot around the pipe to adjust the speed. Although the author used the above method to simulate, but did not analyze the results of the realization [1]. Soon-Joe proposed a cleaning robot motion mode method based on grammatical evolution. The optimization program is generated by using the motion mode grammar defined by the Backus-Naur form. In addition, in the process of program creation, conditional probabilities are used between each syntax element. However, after the simulation evaluation of the robot, it is found that the proposed method is not superior to the comparison algorithm. At present, the aging problem is becoming more and more serious, and the demand for nursing is increasing year by year. Nursing robot is a solution to meet the demand [2]. Kawai R developed a controllable, movable, low-cost nursing robot through the operator's hand movements and conducted an evaluation to verify its effectiveness. At first, the experiment participants felt that they could not operate the robot the way they wanted, but eventually they were able to do it the way they wanted. The disadvantage is that with regard to the robot arm, some participants find it difficult to control it with the developed controller [3].

The innovations of this paper are as follows: (1) The research on the robot less planning method and the robot positioning technology is carried out. (2) An active general positioning algorithm based on real-time positioning function is proposed. (3) Experiments are carried out on the big data-driven robot walking route and real-time positioning intelligent judgment cloud computing.

2. Big Data-Driven Robot Walking Route and Real-Time Positioning Intelligently Determine Cloud Computing Research Methods

2.1. Robot Gait Planning Method. The earliest surviving robot is a teenage doll from the Historical Museum in Nusatier, Switzerland. It was made 200 years ago. The ten fingers of two hands can press the keys of the organ to play music, and it is also played regularly for visitors to enjoy, showing the wisdom of the ancients. Compared with developed countries such as the United States and Japan, the exploration time for biped robots in our country is shorter, and most of them started in the mid-1980s. Among them, Tsinghua University, Harbin Institute of Technology, National University of Defense Technology, Beijing Institute of Technology, and other universities have done a lot of research in this field [4, 5]. Robots can improve social efficiency. The application of robots reduces the workload of human beings and solves some problems that humans cannot solve. For example, Ali's city brain can optimize the time allocation of intersections, improve traffic efficiency, and make busy cities more intelligent. Although it started late compared to other countries, due to the gradual improvement of my country's economic strength and scientific research level, on the other hand, government departments are paying more and more attention to robots. Our country has obtained certain results and experience in the field of biped robots and launched our country's own advanced biped robot [6]. In the 1980s, National Science and Technology University embarked on the development of biped robots and successively developed KWD-1, KWD-2, and KWD-3. Then, in 2000, the country's first biped robot "Forerunner" was developed [7, 8], as shown in Figure 1.

The forerunner can realize most of the actions of ordinary people, such as turning, forwarding, backing up, and going upstairs. And in the following years, the National University of Science and Technology introduced a new generation of robot pioneers, which are basically similar to humans in terms of appearance and function [9]. At present, domestic and foreign researchers have many methods to study the dual-robot hiking plan, but the general methods are similar [10].

2.2. Robot Positioning Technology. The most basic requirement for robots to perform autonomous operations is to have reliable positioning performance. Its direct performance is the ability to accurately obtain the current position coordinates of the robot in the global coordinate system [11]. According to various methods of sensor information fusion, the existing positioning methods for mobile robots can be roughly divided into the following three types. Relative positioning: refers to the offset of the element relative to the original position of the document layout; absolute

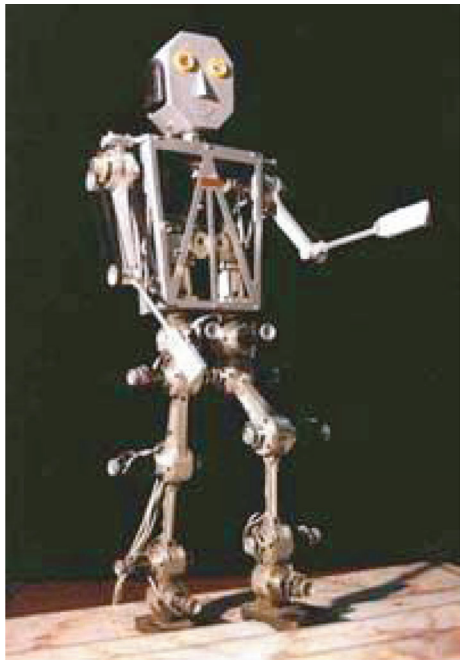

Figure 1: Forerunner robot (this picture is borrowed from Baidu Encyclopedia).

positioning: refers to the arbitrary positioning of the element in the original page separation.

(1) Relative positioning method

It measures the current posture of the robot by measuring the distance and direction of the movement relative to the initial posture based on the built-in sensors of the robot (such as odometer and penetrating navigation) [12]. This method will accumulate inevitable path errors, which will increase with the increase of time and distance, but at the same time, it needs to take the initial stop as a reference and is not suitable for general positioning of robots. Relative positioning methods can be divided into static relative positioning and static relative positioning.

(2) Absolute positioning method

The central idea is to use artificial road signs, active or passive signs, map matching points, or global positioning systems to place them immediately. Position calculation methods include algorithms for trimming, triangulation, or model matching. This type of method has many environmental requirements and usually requires manual changes to the environment, resulting in high maintenance costs. At the same time, certain matching algorithms are slowing down. The concept of absolute positioning is mainly divided into two types: the first is satellite absolute positioning, and the second is absolute positioning in CSS positioning.

(3) Combined positioning method

It is a combination of the first two methods. Taking into account the shortcomings of the first two positioning methods, most portable robot positions are now based on a combination of trajectory estimation and absolute information correction, that is, a combination of positioning methods [13].

2.3. Fisher's Information. Fisher's information is a measure of the amount of information an observable random variable X carries about unknown parameters of the distribution of a model X. Variance is evaluated by mathematical statistics of information, that is, information variance will have a certain impact. To evaluate this impact, we can rely on Fisher's information, which has been verified in mathematical statistics and information theory [14, 15]. People often misunderstand that the prior probability determines the asymptotic distribution of the posterior probability, but this is a misunderstanding. It is Fisher's information that determines the asymptotic distribution of posterior probability. This fact can be obtained by the Bernstein-von Mises theorem in Bayesian statistics [16, 17]. This also shows that Fisher's information plays an important role in the maximum likelihood estimation of asymptotic theory. By extension, the robot's observation information is z, and its possible pose is p. We know that the distribution of z is closely related to p, and Fisher's information can be used to connect the observation information z with the possible pose p relationship [18].

Specifically, the likelihood function of p is represented by $f(z;p)$. When a certain value of p is given, assuming a random variable z corresponds to it, then the probability density of z can be represented by the likelihood function $f(z;p)$, which is the likelihood intuitive explanation of the function. For the likelihood function, first take its natural logarithm; and then obtain the partial derivative of the pose, a function similar to the nature of the score (Score) can be obtained. Under certain conditions (these conditions are regular and follow-able), the scoring consists of two parts, one is the part with a score of 0, and the other non-zero part is defined as Fisher's information:

$$\mathfrak{I}(p) = E\left[\left(\frac{\partial}{\partial p}\log f(z;p)\right)^2 \middle| p\right]. \tag{1}$$

In the above formula, for any given p value, the expression $E[\bullet|p]$ represents the conditional expectation of z in the probability density function $f(z;p)$, where $0 \le \mathfrak{I}(p) < \infty$, and it can also be seen that the absolute value of the score is proportional to Fisher's information [19]. It should be noted that the observation function targeted by Fisher's information here is not specific, and the random variable z can reflect any situation. Furthermore, we pointed out that when the score is 0 as the expectation, then its variance or covariance can be represented by Fisher's information [20, 21].

If there is a precondition, that is, $\log f(z;p)$ is two-order derivable to p, then Fisher's information can be expressed by the following formula under some specific conditions:

$$\mathfrak{I}(p) = -E\left[\frac{\partial^2}{\partial p^2}\log f(z;p) \middle| p\right]. \tag{2}$$

This formula shows that Fisher's information can also be obtained by inverting the natural logarithm of the probability density function $f(z;p)$ to the second derivative of p. It can be seen that this expression reflects the curvature of the curve and can be very conveniently used to evaluate the curve corresponding to the likelihood estimation function of p. When the curve is relatively convex, it is reflected in the larger second-order partial derivative and larger Fisher's information; on the contrary, when the curve is relatively flat, it is reflected in the smaller second-order partial derivative and smaller Fisher's information.

If there is no correlation between the two sets of observations, the sum of the amount of information obtained from each observation is the same as the total amount of information obtained from the two observations [22, 23]. Fisher's information also follows this cumulative property, which is a very good property for the application of this article, which is expressed by the formula:

$$\mathfrak{J}_{z_1,z_2}(p) = \mathfrak{J}_{z_1}(p) + \mathfrak{J}_{z_2}(p). \tag{3}$$

The above results can be proved by the following derivation: the variance of the sum of the variables obtained by adding the random variables is equal to the sum of the variances of each variable, if and only if these random variables are independent of each other, that is: if a random sample of the size is 1, and there is another random sample with the same attribute, and its size is n, so the result of sampling n times in the former and 1 sampling in the latter is the same.

2.4. Cramer-Rao Bound Inequality. From the introduction in the previous section, we can know that in the related asymptotic theory based on maximum likelihood estimation, the amount of information can be obtained from the probability density distribution of the parameters, and this can be described by Fisher's information, which is a very meaningful one thing [24, 25]. In particular, we can find the lower limit of information estimation through CRB inequality. The following is a brief introduction to CRB inequality [26].

The CRB inequality was proposed by Harald Cramér and Calyampudi Radhakrishna Rao. This inequality can be used to determine the lower bound of the estimated variance (covariance) of the parameters. Combining the background of robot positioning, the derivation method of the classic CRB inequality is given below [27, 28].

Assuming that p is an unknown certain pose, it can be estimated by observing the z, and $f(z;p)$ is the probability density function corresponding to observing z. Then, when we estimate the pose p, Fisher's information $\mathfrak{J}(p)$ will reflect the limitation of the value range of its variance (covariance), namely:

$$Var(\hat{p}) \geq \frac{1}{\mathfrak{J}(p)}. \tag{4}$$

Among them, the validity of Fisher's information $\mathfrak{J}(p)$ unbiased estimation is defined as follows:

$$e(\hat{p}) = \frac{\mathfrak{J}(p)^{-1}}{Var(\hat{p})}. \tag{5}$$

It can be seen that the range of $e(\hat{p})$ is (0,1], $Var(\hat{p})$ represents the true variance (covariance), and $\mathfrak{J}(p)^{-1}$ represents the minimum variance (covariance) of the unbiased estimate. We can use the ratio of the two, that is, $e(\hat{p})$ to express the estimator. The minimum variance of that is the lower bound of variance, and the difference between its actual variance (covariance).

The derivation process is as follows: usually, the parameter p that cannot be directly obtained can only be estimated by the observation z, and the parameter p determines the current value of the observation z. We know that due to measurement errors and other factors, the observations z must also have errors and have certain uncertainties. Therefore, in order to link the two together, a probability distribution function $p(z|p)$ needs to be introduced into the parameter p and the observation z. Let the estimated information $T(z)$ of p be the real function of the measured data z, let $\Delta T = T(z) - T_p$, where:

$$T_L = \int p(z|p)T(z)dz. \tag{6}$$

If $T_p = p$ is estimated on average, it is called unbiased estimation. For unbiased estimation, any T and m independent observations $z_1, z_2, \cdots, z_m$ have:

$$\int p(z|p) \cdots p(z_m|p)\Delta T dz_1 \cdots dz_m = 0. \tag{7}$$

To find the partial derivative of p in the above formula, we get:

$$\sum_{i=1}^{m} \int p(z_1|p) \cdots p(z_m|p) \frac{1}{p(z_i|p)} \frac{\partial p(z_i|p)}{\partial p} \Delta T dz_1 \cdots z_m - \frac{dT_p}{dp} = 0. \tag{8}$$

Because p is dependent on T_p instead of T, the above formula can be converted to:

$$\int p(z_1|p) \cdots p(z_1|p) \frac{1}{p(z_i|p)} \left(\sum_{i=1}^{m} \frac{\partial \ln p(z_i|p)}{\partial p} \right) \Delta T dz_1 \cdots dz_m - \frac{dT_p}{dp} = 0. \tag{9}$$

Using Cauchy-Schwarz inequality

$$\left[\int f(x)g(x)dx \right]^2 \leq \int f(x)^2 dx \int g(x)^2 dx. \tag{10}$$

Available:

$$\int p(z_1|p)\cdots p(z_m|p)\left(\sum_{i=1}^{m}\frac{\partial \ln p(z_i|p)}{\partial p}\right)^2 dz_1\cdots dz_m \times \int p(z_1|p)\cdots p(z_m|p)(\Delta T)^2 p(z_1|p)\cdots p(z_m|p) \geq \left|\frac{dT_p}{dp}\right|^2. \tag{11}$$

Introduce Fisher's information $\mathfrak{I}(p)$ and get 引入 Fisher's 信息 $\mathfrak{I}(p)$,

$$m\mathfrak{I}(p)(\Delta T)^2 \geq \left|\frac{dT_p}{dp}\right|^2. \tag{12}$$

For the unbiased estimator, $(\Delta T)^2$ is the variance (covariance) square $Var(\widehat{p})^2$ of the estimated pose $\widehat{p}$, and $dTp/dp = 1$, the CRB inequality can be finally obtained.

The CRB inequality uses the inverse of Fisher's information to give the smallest variance (covariance) that may occur when estimating the pose. It can be seen that the smaller Fisher's information indicates the lack of observational information in the pose, which means that the estimation of the current pose is biased, and the measurement variance (covariance) is larger. Therefore, the amount of observation information is crucial to whether a parameter can be accurately estimated. Based on people's basic cognition, the more information, the more accurate the estimation result will be. What needs to be explained here is that Fisher's information is usually in the form of a matrix, because the parameters that need to be estimated often contain multiple variables; in addition, the lower limit of the variance (covariance) calculated by the CRB inequality is only theoretical. The actual variance (covariance) usually deviates from the theoretical value. This is due to the different methods of evaluating parameters through observation information, the error or lack of observation information, etc., but this deviation is usually within the allowable range.

2.5. Discretization Observation Model. In recent years, in the research of mobile robot positioning, scholars generally believe that it is an effective positioning method to correct the error of the odometer through the sensor to perceive the surrounding environment, and it has had many successful practical applications [29, 30]. The algorithm used in this paper is a laser rangefinder that perceives the distance of the environment. The laser observation model is shown in Figure 2:

The pose of the robot is expressed by $p_t = [x_t, y_t, \theta_t]$, $r_{iE}(p_t, \phi_i)$ is the expected distance scanned by the i laser ray, and the total number of laser rays is N_o. Then, the laser observation model equation can be defined as:

$$r_i = r_{iE}(p_t, \phi_i) + \varepsilon_i, i = 1, 2, \cdots, N_o. \tag{13}$$

Among them, ε_i represents Gaussian random noise with a mean value of 0 and a variance of σ_i^2. In practical applications, the analytical map of the real environment is usually not available. Therefore, r_{iE} cannot be accurately calculated. ε_i is a partial item that reflects physical influence factors, such as robot speed, obstacle distance, orientation, and surface material. Therefore, ε_i and its variance σ_i^2 cannot be directly calculated.

3. Big Data-Driven Robot Walking Route and Real-Time Positioning Intelligently Determine Cloud Computing Experiments

3.1. The Positioning and Environment Construction of Mobile Robots

(1) Positioning

The positioning system is designed for a specific location and should describe the characteristics of the environment. Most positioning systems operate in a structured environment, but other positioning systems rely on GPS for placement, so they can only operate in an outdoor environment. Some robots need to make real-time mapping anytime and anywhere, while other robots only need to be placed on the map created by the robot.

For indoor installation systems, most positioning algorithms come from indoor installation systems. In a structured environment, it is necessary to simplify the structure of the environment, such as a flat ground, without considering the obstacles of potholes. These methods are to align external objects such as doors and glass to determine their location and orientation.

The outdoor installation system uses GPS as the main installation method for outdoor robots. However, GPS may not always be able to receive enough satellite signals. In other words, GPS cannot produce accurate results. This requires the use of other sensors (such as rangefinders) to improve system accuracy and correct GPS errors.

Indoors and outdoors, there are few methods that can be used in both environments at the same time. This is because indoor methods are highly structured environments and therefore not suitable for outdoor work. In addition, GPS does not work indoors. It is difficult to find a suitable method indoors and outdoors. In addition to using signs in the environment, cameras can also be used to capture the terrain and structure of the environment using positioning methods based on surface features.

(2) Map construction

For the positioning problem, there are two ways to build a map. Under normal circumstances, it is to complete the construction of the map before the implementation of positioning. Another way is to continuously complete the map as the robot moves in the environment, that is, SLAM.

SLAM is the main research topic of robotics. These methods can help robots run in unknown environments and display the number of robots running on service robots (such as wheelchair robots, cleaning robots, and search and rescue robots).

In order to realize the construction of the robot map, it is necessary to solve some problems of communication, dynamic environment, and robot search. Communication problems refer to the consistency of information detected

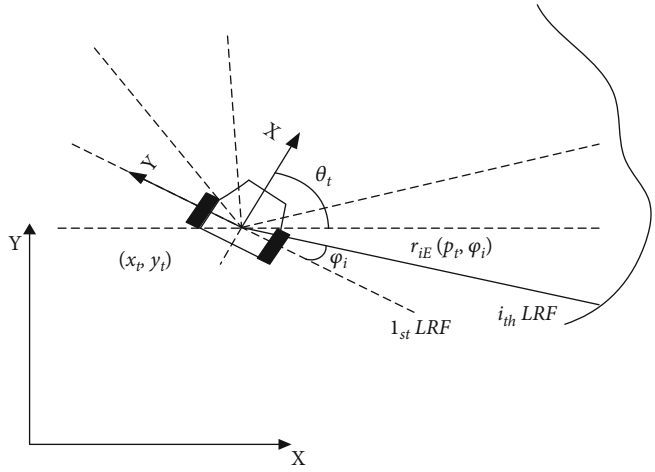

Figure 2: Laser observation model.

Table 1: Judgment conditions for different convergence states.

State of convergence	Judgment condition
a	(1) More than 80% of the particles converge to 10 convergent cluster centers (2) M_p>10 grids, and M_r>10 grids
A	(1) More than 80% of the particles converge to 10 convergent cluster centers (2) M_p<2 grids, and M_r<2 grids
B	(1) More than 80% of the particles converge to 10 convergent cluster centers (2) M_p<2 grids, and M_r>20 grids

by different sensors on the same object. The dynamic environment includes moving objects such as people and cars, and other factors also cause natural changes. Robot exploration is the function of robots navigating while mapping the map. The advantage of this method is that the robot can be placed in an environment that has not been visited before, the environment map is constantly changing, and the robot can also be placed in a changing environment.

3.2. Simulation Test. For simulation, the hardware platform is an Intel personal computer (Intel Core2 Duo E7200 2.5G CPU, DDR2-800 2G RAM). For the experiment, the hardware platform is the "Jiao-long" smart wheelchair independently developed by the laboratory. On the "Jiao-long" wheelchair platform, the positioning algorithm is executed on an industrial computer (Intel Core Duo T2500 2.0G CPU, DDR2-667 3G RAM); the wheelchair adopts two-wheel differential drive, and the controller is self-designed DSP motion control board; meanwhile, the wheelchair is equipped with an odometer, which is calibrated in advance, and equipped with a laser rangefinder (SICK LMS111).

For simulation and experiment, the software platform uses CARMEN, an open source robot simulation platform under Linux SUSE system. When comparing different positioning algorithms, standard algorithms, such as the standard particle filter algorithm with "roulette" re-sampling process, are implemented based on CARMEN standard code; and for improved algorithms based on positioning capabilities, and other needs to be compared. The algorithm is implemented by the secondary development of the standard code under CARMEN. For smart wheelchairs, the main sensors are odometer and laser rangefinder. The errors brought by these sensors will inevitably have an impact on the algorithm. In the following, how to simulate these sensor errors in the simulation will be specifically explained. The odometer uses a photoelectric encoder to record the mileage data. Although it has been pre-calibrated, it still has a certain error. Mainly include system errors such as small precision errors, driver errors, and non-system errors caused by wheel slip caused by uneven road surface. In addition, as the weight of the user carried by the "Jiao-long" smart wheelchair is different, the deformation of the wheel changes, and its kinematics model will also change to a certain extent.

For active global positioning algorithms based on positioning capabilities, before simulation and experimentation, a global probability grid map needs to be established first. Furthermore, based on the known map, the positioning ability in each pose can be calculated offline in advance and stored. Because the laser rangefinder used in this article is not omnidirectional scanning, when we calculate the positioning capability offline, we need to discretize the observation direction, that is, to discretize a different observation direction. In addition, the greater the system sampling interval, the greater the sensor error introduced. Therefore, this

Table 2: Simulation and experimental parameters of the global positioning algorithm.

Description	Parameter
Map resolution (raster size)	$0.1 \times 0.1m^2$
Static positioning capability discrete step size	$\Delta x = \Delta y = 0.1m, \Delta\theta = 1^\circ$
Maximum scanning distance of laser rangefinder	$D_{\max} = 20m$
Laser rangefinder scanning range, resolution, and number of rays	$0 - 180\circ, 1\circ, N_o = 181$
Simulated odometer error	$[10\circ/m10cm/m20\circ/360\circ]$
Number of actions	$N_a = 5$
Linear velocity of motion	$\vec{v} = 0.4m/s$
Linear velocity coefficient	$k_v = 1.0$
Angular velocity of action	$\vec{w} = 20\circ/s$
Angular velocity coefficient	$k_w = 1.0$
Action execution time	$\Delta t = 2.0s$
High weight judgment threshold	$w_t^{(k)} = 0.7$

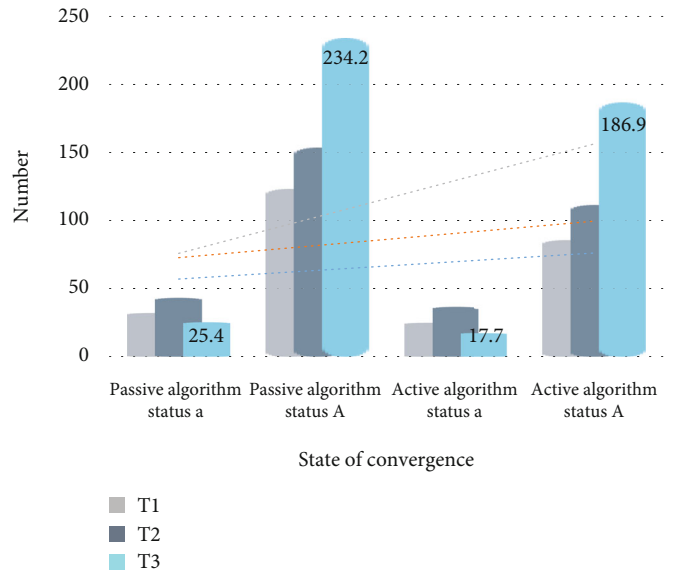

Figure 3: Comparison of average convergence steps between active and passive global positioning algorithms.

article sets the effective sampling time of the simulation to 400 ms in order to reserve the necessary and possible sampling time consumption for future practical applications.

In the simulation, we can know the real pose of the robot, so we can make good use of it when analyzing the simulation results (here the real robot pose is not used in the active global positioning algorithm, but only used for the analysis of the positioning results). Specifically, based on the real robot pose, K-mean algorithm, and Mahalanobis distance (Mahalanobis distance), the convergence state of the particles can be clearly classified. The particle convergence state a indicates that the pre-convergence has been completed, and the particles have been clustered into several more obvious particle piles; the particle convergence state A indicates that most of the particles are clustered into one particle pile, and the estimated robot pose and the real robot position the pose is close; the particle convergence state B indicates the state of convergence failure, that is, although most of the particles are clustered into a particle pile, the robot pose estimated by the particles is the judgment condition of three different convergence states that deviate from the real robot pose as shown in Table 1:

Table 3: Comparison of active and passive global positioning algorithm state B.

Cycle	Passive algorithm status B	Active algorithm status B
T1	2/80	0/80
T2	15/80	6/80
T3	49/80	28/80

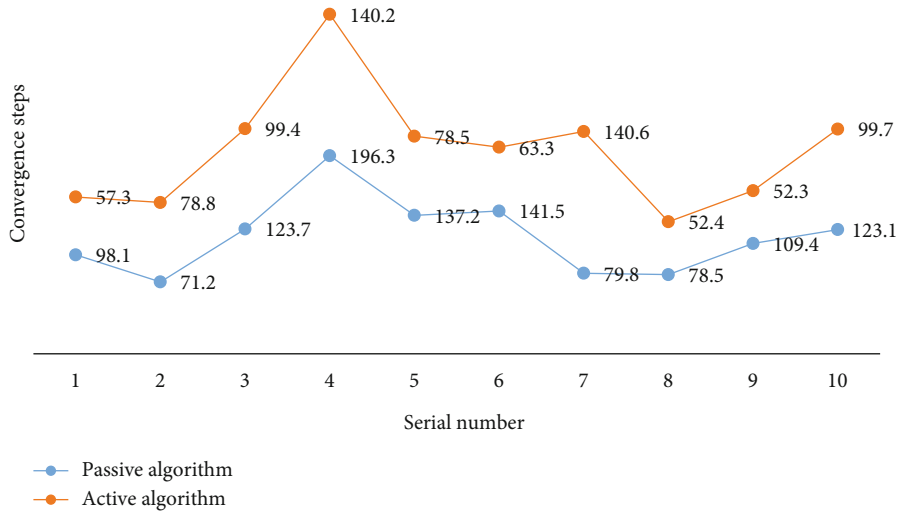

Figure 4: T1 area simulation serial number.

In Table 1, M_p is the Mahalanobis distance between the center point of all convergent clusters and the estimated pose of the robot; M_r is the Mahalanobis distance between the center point of the convergent cluster and the real pose of the robot; one of the grids represents 0.1 m. In addition, the parameters used in the simulation and experiment of the global positioning algorithm (including the required number of particles, etc.) are given below, as shown in Table 2.

4. Big Data-Driven Robot Walking Route and Real-Time Positioning Intelligent Determination of Cloud Computing Experimental Analysis

In the simulation, the algorithm based on the positioning capability proposed in this paper was compared in a wide range of environments and in different scenarios, with all parameters (such as the number of particles, etc.) and the simulation environment of different scenarios. In comparison, the scene has a small number of environmental structures with unclear geometric characteristics and a number of map noises, but looking at the global map, its observation characteristics are relatively clear; the scene is an office, and looking at the global map, its observation characteristics are relatively similar. And there are many environmental structures and map noises with unclear geometric features; scene T3 is a corridor. Although there are not many environmental structures and map noises with unclear geometric features, the observation features are very similar in the global map. The location is very easy to introduce observational ambiguity.

Because the laser rangefinder used in this article does not observe omnidirectionally for different scenarios, 4 sets of simulations are carried out based on four different initial orientations of "UP," "DOWN," "LEFT," and "RIGHT"; contain 20 comparison simulations; one comparison is composed of two simulations based on passive and active global positioning algorithms. These two simulations based on different algorithms are used for comparison, and their initial conditions, such as the initial pose of the real robot and the initial particle distribution., are completely the same; in addition, in order to collect statistical data, the initial conditions of the 20 different comparisons in each group are independent of each other and randomly generated.

According to the defined particle convergence state, during the convergence process, the particle generally converges to the state a first, and secondly, the particle may converge to the state A or B. Of course, during the convergence process, there is also a certain probability that it will not go through the transition state a, but will directly converge to the state A or B. As mentioned above, state A indicates correct convergence, and state B indicates an incorrect convergence result. In the simulation, statistical methods are used to analyze the results. Figure 3 shows the average number of convergence steps in different scenarios.

For state B, the number of convergence failures is recorded and compared, as shown in Table 3.

It can be seen from Figure 3 that no matter in which scenario, the average number of steps the algorithm proposed in this paper converges to states a and A is more efficient than the passive algorithm. Scenario T2, especially T3, brings a lot of ambiguity to the robot observation. For passive algorithms, it is easy to fail to converge in these scenarios. For example, in T3, a total of 80 simulations failed 49 times, and in the application proposed in this article algorithm, the number of failures is reduced to 28. The above results show that the algorithm proposed in this paper effectively accelerates the convergence speed of global positioning due to the influence of known map uncertainty on global positioning and does not specifically extract a clear environment during the application of positioning capabilities to determine robot movements and features to ensure the practical application ability and real-time performance of the algorithm. At the same time, this also shows that the algorithm proposed in this paper has strong robustness for

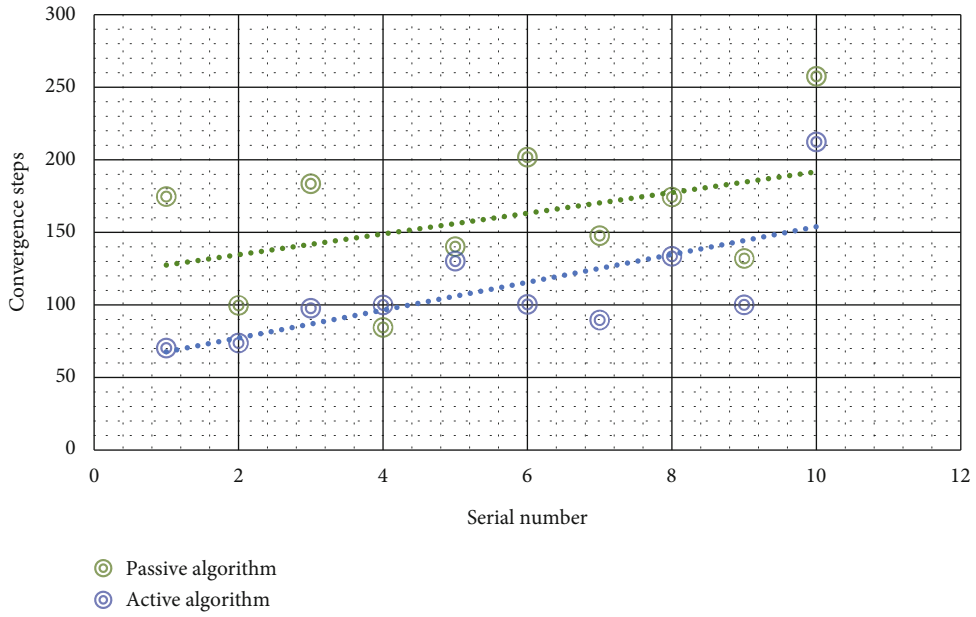

Figure 5: T2 area simulation serial number.

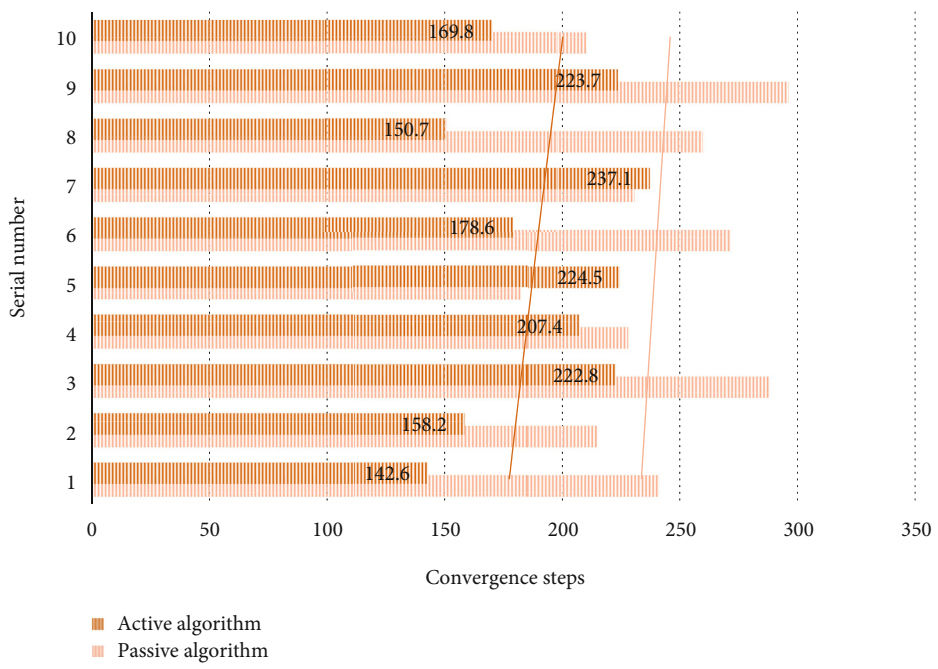

Figure 6: T3 area simulation serial number.

different scenes with fuzzy geometric features and different map noise levels.

The data of each simulation sequence number in scenario T1 is shown in Figure 4:

The data of each simulation sequence number in scenario T2 is shown in Figure 5:

The data of each simulation serial number in scene T3 is shown in Figure 6:

Figures 4–6 compare the number of steps taken by different algorithms to converge to the state through statistical graphs. These data are randomly selected from all the simulations that successfully converged. Figures 4–6 are data in different scenarios. It can be seen that in most cases, the algorithm proposed in this paper converges faster than the passive algorithm. The data clearly shows the advantages that the global positioning algorithm brings to the global positioning algorithm taking into account the uncertainty of the known map (included in the positioning capability estimation): the convergence of the global positioning is accelerated speed and enhances the robustness of the algorithm.

5. Conclusions

The robot itself is a non-linear object with strong coupling and contains many uncertainties. When the final operating robot is in contact with the external environment, the working environment will also significantly affect the performance of the control. In the real-time positioning and walking route of mobile robots, in addition to the measurement errors or performance limitations of its own sensors, the construction noise of known maps, the actual environment lacking clear geometric features, dynamic obstacles, data fusion, and real-time algorithmic factors, both will bring uncertainty to the positioning of mobile robots. This article is to analyze the impact of some or all of the abovementioned uncertain factors on the positioning and walking route of the mobile robot and improve the positioning algorithm. Through simulation and experimental results, it is verified in the actual environment. Algorithm compared with the passive general positioning algorithm, the algorithm in this paper speeds up the convergence of general positioning in the experiment. At the same time, by comparing with the experimental results of the existing active global positioning algorithm, it can be seen that the active global positioning algorithm based on the positioning ability proposed in this paper has a great advantage in computational efficiency; especially for the active global positioning whose core idea is similar to this paper as far as the algorithm is concerned, it can be seen that the improvement effect is more obvious. However, due to the limitations of time and technology, this paper does not conduct a more in-depth discussion of robot positioning, and we will further discuss this in the follow-up.

Data Availability

Data sharing was not applicable to this article as no datasets were generated or analyzed during the current study.

Conflicts of Interest

The authors declare that there is no conflict of interest with any financial organizations regarding the material reported in this manuscript.

References

[1] A. Rezaee, "Determining PID controller coefficients for the moving motor of a welder robot using fuzzy logic," *Automatic Control & Computer ences*, vol. 51, no. 2, pp. 124–132, 2017.

[2] S. J. Gwon, H. T. Kim, and C. W. Ahn, "Designing the moving pattern of cleaning robot based on grammatical evolution with conditional probability table," *KIISE Transactions on Computing Practices*, vol. 22, no. 4, pp. 184–188, 2016.

[3] R. Kawai and T. Arakawa, "Trial development of nursing care robot moving by intuitive hand motion," *International Journal of Innovative Computing Information and Control*, vol. 15, no. 6, pp. 2109–2118, 2019.

[4] X. Li and R. Fung, "Optimal K-unit cycle scheduling of two-cluster tools with residency constraints and general robot moving times," *Journal of Scheduling*, vol. 19, no. 2, pp. 165–176, 2016.

[5] M. Nakajima, K. Tanaka, and F. Matsuno, "Motion control of a snake robot moving between two non-parallel planes," *Advanced Robotics: The International Journal of the Robotics Society of Japan*, vol. 32, no. 10, pp. 559–573, 2018.

[6] J. Kim and J. Chung, "Dynamic analysis of an axially moving robot manipulator supported by bearings," *Journal of Mechanical Science and Technology*, vol. 31, no. 7, pp. 3143–3155, 2017.

[7] T. Yamamoto, M. Konyo, K. Tadakuma, and S. Tadokoro, "A flexible in-pipe robot capable of moving in open spaces via a pneumatic rotary mechanism," *Ifac Papersonline*, vol. 50, no. 1, pp. 1050–1055, 2017.

[8] C. H. Chang, S. C. Wang, and C. C. Wang, "Exploiting moving objects: multi-robot simultaneous localization and tracking," *IEEE transactions on automation science and engineering: a publication of the IEEE Robotics and Automation Society*, vol. 13, no. 2, pp. 810–827, 2016.

[9] J. H. Cho, E. H. Jung, J. Y. Kim, M. H. Park, and Y. T. Kim, "A study on improved navigation algorithm of logistics transportation robot for freight moving on the rack," *Journal of Korean institute of intelligent systems*, vol. 28, no. 5, pp. 436–442, 2018.

[10] C. Liu, "Safe robot navigation among moving and steady obstacles [bookshelf]," *IEEE Control Systems*, vol. 37, no. 1, pp. 123–125, 2017.

[11] K. S. Yoon, M. S. Lee, and Y. W. Sung, "A study on an omnidirectional mobile robot for moving a double-parked car," *Transactions of the Korean Institute of Electrical Engineers*, vol. 67, no. 3, pp. 440–447, 2018.

[12] M. Roozegar and M. J. Mahjoob, "Modelling and control of a non-holonomic pendulum-driven spherical robot moving on an inclined plane: simulation and experimental results," *Iet Control Theory & Applications*, vol. 11, no. 4, pp. 541–549, 2017.

[13] M. Sharifnia and A. Akbarzadeh, "Dynamics and vibration of a 3-PSP parallel robot with flexible moving platform," *Journal of Vibration and Control*, vol. 22, no. 4, pp. 1095–1116, 2016.

[14] Z. L. Ma, P. Q. Zhang, and R. J. Lü, "Mass center adjustment method of quadruped robot moving on slopes," *Beijing Ligong Daxue Xuebao/Transaction of Beijing Institute of Technology*, vol. 38, no. 5, pp. 481–486, 2018.

[15] T. Weingartshofer, M. Schwegel, C. Hartl-Nesic, T. Glück, and A. Kugi, "Collaborative synchronization of a 7-Axis robot," *IFAC-Papers OnLine*, vol. 52, no. 15, pp. 507–512, 2019.

[16] S. Zhao, Z. Zhang, D. Xiao, and K. Xiao, "A turning model of agricultural robot based on acceleration sensor," *IFAC-Papers OnLine*, vol. 49, no. 16, pp. 445–450, 2016.

[17] A. Rutkin, "Robot guard powerless to stop food thieves," *New Scientist*, vol. 231, no. 3090, pp. 24–24, 2016.

[18] E. I. Barakova, P. Bajracharya, M. Willemsen, T. Lourens, and B. Huskens, "Long-term LEGO therapy with humanoid robot for children with ASD," *Expert Systems the Journal of Knowledge Engineering*, vol. 32, no. 6, pp. 698–709, 2015.

[19] B. Gao, Z. Zhu, J. Zhao, and L. Jiang, "Inverse kinematics and workspace analysis of a 3 DOF flexible parallel humanoid neck robot," *Journal of Intelligent & Robotic Systems*, vol. 87, no. 2, pp. 211–229, 2017.

[20] J. Kim, "Path plan strategy of an underwater robot to approach a moving emitter while maximising sound intensity measurements," *IET Radar Sonar & Navigation*, vol. 13, no. 5, pp. 795–801, 2019.

[21] J. M. Kim, J. K. Son, and S. J. Wan, "Development of robot's vision control scheme using the data moving method for the tracking of moving target," *Journal of the Korean Society for Precision Engineering*, vol. 35, no. 7, pp. 669–679, 2018.

[22] S. K. Han, S. Y. Chung, and M. J. Hwang, "A study on motion acceleration-deceleration time to suppress residual vibration of robot," *The Journal of Korea Robotics Society*, vol. 12, no. 3, pp. 279–286, 2017.

[23] S. Saeedi, M. Trentini, M. Seto, and H. Li, "Multiple-robot simultaneous localization and mapping: a review," *Journal of Field Robotics*, vol. 33, no. 1, pp. 3–46, 2016.

[24] S. Kazemi and H. Kharrati, "Visual processing and classification of items on moving conveyor with pick and place robot using PLC," *Intelligent Industrial Systems*, vol. 3, no. 1, pp. 15–21, 2017.

[25] A. A. Mohammed, I. Aris, M. K. Hassan, and N. A. Kamsani, "New algorithm for autonomous dynamic path planning in real-time intelligent robot car," *Journal of Computational and Theoretical Nanoscience*, vol. 14, no. 11, pp. 5499–5507, 2017.

[26] M. Stommel and W. Xu, "Learnability of the moving surface profiles of a soft robotic sorting table," *IEEE Transactions on Automation Science & Engineering*, vol. 13, no. 4, pp. 1581–1587, 2016.

[27] B. Shin, Y. Kim, J. Paik, and K. M. Lee, "Miniaturized twin-legged robot with an electromagnetic oscillatory actuator," *Journal of Bionic Engineering*, vol. 15, no. 1, pp. 106–113, 2018.

[28] X. Wang, "Design and kinematics analysis of transformable wheel-legged robot," *Journal of Computational and Theoretical Nanoscience*, vol. 13, no. 11, pp. 8158–8164, 2016.

[29] R. E. Sánchez-Alonso, J. J. González-Barbosa, E. Castillo-Castañeda, and M. A. García-Murillo, "Análisis Cinemático de un Novedoso Robot Paralelo Reconfigurable," *Revista Iberoamericana de Automática e Informática Industrial RIAI*, vol. 13, no. 2, pp. 247–257, 2016.

[30] X. Dai, L. Jiang, and Z. Yan, "Cooperative exploration based on supervisory control of multi-robot systems," *Applied Intelligence*, vol. 45, no. 1, pp. 18–29, 2016.